

RE: A point-to-point response to reviewers' comments

“A proxy for atmospheric daytime gaseous sulfuric acid concentration in urban Beijing” (acp-2018-1132) by Yiqun Lu, Chao Yan, Yueyun Fu, Yan Chen, Yiliang Liu, Gan Yang, Yuwei Wang, Federico Bianchi, Biwu Chu, Ying Zhou, Rujing Yin, Rima Baalbaki, Olga Garmash, Chenjuan Deng, Weigang Wang, Yongchun Liu, Tuukka Petäjä, Veli-Matti Kerminen, Jingkun Jiang, Markku Kulmala, Lin Wang

We are grateful to the helpful comments from Dr. Santtu Mikkonen, and have carefully revised our manuscript accordingly. A point-to-point response to the comments, which are repeated in italic, is given below.

In addition to the reviewers' comments, we have noticed and corrected a key typo from our previous version of manuscript. “The [NO₂] concentration” in our manuscript is in fact “the [NO_x] concentration”. Correction of this term does not lead to changes in our conclusions.

Santtu Mikkonen's comments:

It is interesting to see how the sulphuric acid concentration can be approximated in highly polluted environment, as we did not have such data when we were making our paper Mikkonen et al. (2011). Even more interesting is, that your recommended proxy N2 is quite close to our second recommendation, simple proxy L3, having SO2 power to 0.5 when you have power of 0.4. In addition, I was surprised that the H2SO4 concentration was not higher than shown in Table 1. We had similar average concentrations in San Pietro Capofiume and considerably higher in Atlanta, even though they are less polluted environments. Could you add a comment on that?

Reply: We are very grateful to the positive viewing of our manuscript by Dr. Santtu Mikkonen, and have now revised our manuscript accordingly.

As Dr. Mikkonen has noticed, Beijing did not in this campaign have a higher average concentration of sulfuric acid than other cities, which can be potentially explained by the fact that, firstly, the averaged condensation sink in Beijing in this campaign is around 0.11 s^{-1} that corresponds to a very efficient removal of gaseous sulfuric acid, and secondly, the SO₂ concentration has dramatic reduced in recent years in Beijing as we have mentioned in L488-L489.

I just want to ask about Figure 4: Why only one day, and not averages over whole period such that uncertainty would also be indicated, is shown in the figure? In addition, why comparison only to Boreal forest-proxy from Petäjä et al, why not to Mikkonen et al., who had data from multiple sites?

Reply: Figure 3 (now updated to a new version) presents a statistical comparison between measured

and predicted sulfuric acid concentrations over the whole period.

We compared our results with the Petäjä *et al.* study instead of the Mikkonen *et al.* study, simply because we only measured the UVB and a correlation between UVB and the global radiation cannot be established.

A minor comment on the use of p-value as a screening factor for correlation (in line 266): it is not recommended. See e.g. Greenland et al. (2016): DOI 10.1007/s10654-016-0149-3

Reply: We removed p-values as a screening factor for correlations. Now all the correlations are shown in Table 2.

1 A proxy for atmospheric daytime gaseous sulfuric acid 2 concentration in urban Beijing

3 Yiqun Lu¹, Chao Yan², Yueyun Fu³, Yan Chen⁴, Yiliang Liu¹, Gan Yang¹, Yuwei Wang¹,
4 Federico Bianchi², Biwu Chu², Ying Zhou⁵, Rujing Yin³, Rima Baalbaki², Olga Garmash²,
5 Chenjuan Deng³, Weigang Wang⁴, Yongchun Liu⁵, Tuukka Petäjä^{2,5,6}, Veli-Matti Kerminen²,
6 Jingkun Jiang³, Markku Kulmala^{2,5}, Lin Wang^{1,7,8*}

7 ¹ Shanghai Key Laboratory of Atmospheric Particle Pollution and Prevention (LAP³),
8 Department of Environmental Science & Engineering, Jiangwan Campus, Fudan University,
9 Shanghai 200438, China

10 ²Institute for Atmospheric and Earth System Research / Physics, Faculty of Science, University
11 of Helsinki, 00014 Helsinki, Finland

12 ³ State Key Joint Laboratory of Environment Simulation and Pollution Control, School of
13 Environment, Tsinghua University, Beijing 100084, China

14 ⁴Institute of Chemistry, Chinese Academy of Sciences, Beijing 100190, China

15 ⁵ Aerosol and Haze Laboratory, Advanced Innovation Center for Soft Matter Science and
16 Engineering, Beijing University of Chemical Technology, Beijing 100029, China

17 ⁶ Joint International Research Laboratory of Atmospheric and Earth System Sciences
18 (JirLATEST), School of Atmospheric Sciences, Nanjing University, Nanjing 210023, China

19 ⁷ Institute of Atmospheric Sciences, Jiangwan Campus, Fudan University, Shanghai 200438,
20 China

21 ⁸ Shanghai Institute of Pollution Control and Ecological Security, Shanghai 200092, China

22 * Corresponding Author: L.W., email, lin_wang@fudan.edu.cn; phone, +86-21-31243568.
23

24 **Abstract.** Gaseous sulfuric acid is known as one of the key precursors for atmospheric
25 new particle formation processes, ~~but its measurement remains a difficulty~~
26 ~~measurement remains a major challenge~~. A proxy method that is able to derive gaseous
27 sulfuric acid concentrations from parameters that can be measured relatively easily and
28 accurately is therefore ~~highly desirable for the atmospheric chemistry community~~
29 ~~highly desirable among the atmospheric chemistry community~~. Although such methods are
30 available for clean atmospheric environments, a proxy that works well in a polluted
31 atmosphere, such as those in Chinese megacities, is yet to be developed. In this study,
32 the gaseous sulfuric acid concentration was measured in February-March, 2018, in
33 urban Beijing by a nitrate based - Long Time-of-Flight Chemical Ionization Mass
34 Spectrometer (LToF-CIMS). A number of atmospheric parameters were recorded
35 concurrently including the ultraviolet radiation B (UVB) intensity, concentrations of O₃,
36 NO_x (sum of NO and NO₂), SO₂ and HONO, and aerosol particle number size

37 distributions. A proxy for atmospheric daytime gaseous sulfuric acid concentration was
38 derived ~~using through~~ a statistical analysis method by using the UVB intensity, [SO₂],
39 condensation sink (CS), [O₃], and [HONO] (or [NO_x]) as the predictor variables. In this
40 proxy method, we considered the formation of gaseous sulfuric acid from reactions of
41 SO₂ and OH radicals during the daytime, and loss of gaseous sulfuric acid due to its
42 condensation onto the pre-existing particles. In addition, we explored formation of OH
43 radicals from the conventional gas-phase photochemistry using ozone as a proxy and
44 from the photolysis of ~~heterogeneously formed~~ HONO using HONO (and subsequently
45 NO_x) as a proxy. Our results showed that the UVB intensity and [SO₂] are dominant
46 factors for the production of gaseous sulfuric acid, and that the simplest proxy could be
47 constructed with the UVB intensity and [SO₂] alone. When the OH radical production
48 from both homogeneously- and heterogeneously-formed precursors were considered, the
49 relative errors were reduced up to 20 %, resulting in up to 29% relative deviations
50 when sulfuric acid concentrations were larger than 2.0×10^6 molecules cm⁻³. ~~When~~
51 ~~the OH radical production from both homogeneously and heterogeneously formed~~
52 ~~precursors were considered, the relative deviations were lower than 24%.~~

53 1 Introduction

54 Gaseous sulfuric acid (H_2SO_4) is a key precursor for atmospheric new particle
55 formation (NPF) processes (Kerminen, 2018; Kirkby et al., 2011; Kuang et al., 2008;
56 Kulmala and Kerminen, 2008; Sipilä et al., 2010). A number of atmospheric nucleation
57 mechanisms including H_2SO_4 - H_2O binary nucleation (Benson et al., 2008; Duplissy et
58 al., 2016; Kirkby et al., 2011), H_2SO_4 - NH_3 - H_2O ternary nucleation (Kirkby et al., 2011;
59 Korhonen et al., 1999; Kürten et al., 2015), and H_2SO_4 -DMA- H_2O ternary nucleation
60 ([Almeida et al., 2013](#); [Jen et al., 2014](#); [Kürten et al., 2014](#); [Petäjä et al., 2011](#); [Yao et al.,](#)
61 [2018](#)) ~~involve~~ demand the participation of gaseous sulfuric acid molecules. In addition,
62 the condensation of gaseous sulfuric acid onto newly-formed particles contributes to
63 their initial growth ([Kuang et al., 2012](#); [Kulmala et al., 2013](#)). Quantitative assessments
64 of the contribution of gaseous sulfuric acid to both the new particle formation rates and
65 the particle growth rates require real-time measurements of gaseous sulfuric acid
66 concentrations ~~prior to and~~ during the NPF events (Nieminen et al., 2010; Paasonen et
67 al., 2010).

68 Measurements of gaseous sulfuric acid in the lower troposphere are challenging
69 because its ambient concentration is typically quite low (10^6 - 10^7 molecule cm^{-3})
70 (Kerminen et al., 2010; Mikkonen et al., 2011). Reported real-time measurements of
71 gaseous sulfuric acid are currently based on Chemical Ionization Mass Spectrometry
72 with NO_3^- ~~and its ligands~~ as reagent ions (nitrate CIMS) because ~~nitrate CIMS with an~~
73 ~~atmospheric pressure interface (API)CIMS~~ has a low detection limit for the
74 atmospheric concentration range of gaseous sulfuric acid (Jokinen et al., 2012), and a
75 constant fraction of sulfuric acid present in the air sample will be ionized by excessive
76 nitrate ions in CIMS under constant instrumental conditions (Kürten et al., 2012; Zheng
77 et al., 2010), which makes the quantification of gaseous sulfuric acid feasible.

78 Arnold and Fabian (1980) measured the negative ions in the stratosphere ~~using a~~
79 ~~passive CIMS~~ and derived the concentration of stratospheric gaseous sulfuric acid from
80 the fractional abundances of a series of stratospheric negative ions as well as the
81 ~~associated equilibrium or~~ rate constants. Later, real-time measurement of sulfuric acid
82 in the lower troposphere was performed using nitrate CIMS (Eisele and Tanner, 1993),
83 with laboratory calibrations by production of known concentrations of OH radicals that
84 ~~will be~~ titrated into gaseous sulfuric acid. Thereafter, measurements of sulfuric acid
85 using CIMS have been performed around the world ([e.g., Berresheim et al., 2000](#);
86 [Bianchi et al., 2016](#); [Chen et al., 2012](#); [Jokinen et al., 2012](#); [Kuang et al., 2008](#); [Kürten](#)

87 [et al., 2014; Kurtén et al., 2011; Petäjä et al., 2009; Weber et al., 1997; Zheng et al.,](#)
88 [2011](#)), and CIMS has been proven~~d~~ to be a robust tool for gaseous sulfuric acid
89 detection. However, sulfuric acid measurements are still rather sparse because of the
90 high cost of the CIMS instrument and the extensive demand of specialized expertise on
91 the instrument calibration, maintenance, and data processing, etc. Therefore, a proxy
92 for gaseous sulfuric acid concentration is highly desirable.

93 Proxies for the estimation of atmospheric gaseous sulfuric acid concentrations
94 were previously developed to approximate measurement results of sulfuric acid
95 in Hyytiälä Southern Finland (Petäjä et al., 2009), ~~assum~~~~suppos~~ing that gaseous
96 sulfuric acid is formed from reactions between SO₂ and OH radicals, and lost due to its
97 condensation onto pre-existing particles. The derived simplest proxy can be written as
98 Eq. (1) below, and the authors recognized that the proxies might be site-specific and
99 should be verified prior to utilization in other environments.

$$101 \quad [H_2SO_4] = k \cdot \frac{[SO_2] \cdot (UVB \text{ or } Global \text{ radiation})}{CS} \quad (1)$$

102
103 Mikkonen et al. (2011) later developed a couple of statistical proxies based on
104 measurements of sulfuric acid in six European and North American sites, including
105 urban, rural and forest areas. Their results showed that the radiation intensity and [SO₂]
106 are the most important factors to determine the concentration of sulfuric acid, and that
107 the impact of condensation sink (CS), ~~a proxy for condensational sink~~ for gaseous
108 sulfuric acid, is generally negligible. In several proxies developed by Mikkonen et al.
109 (2011), the correlation between the gaseous sulfuric acid concentration and CS is
110 positive, which is against what one would expect because a larger CS normally leads
111 to a faster loss for gaseous sulfuric acid. In addition, the performance of a proxy
112 equation is site-specific because of varying atmospheric conditions from one site to
113 another, which implies that the proxy suggested by Mikkonen et al. (2011) might not
114 work well in locations ~~that characterized~~ ~~with an~~ atmospheric environments~~s~~ different
115 from those in the six sites of that study.

116 Beijing is a location with typical values of CS (e.g., 0.01-0.24 s⁻¹ in the 5-95%
117 percentiles in this study) being 10-100 times higher (Herrmann et al., 2014; Wu et al.,
118 2007; Xiao et al., 2015; Yue et al., 2009; Zhang et al., 2011) and typical SO₂
119 concentrations being 1-10 times higher (Wang et al., 2011a; Wu et al., 2017) than those

120 in Europe and North America ([Dunn et al., 2004](#); [Mikkonen et al., 2011](#)), yet measured
121 gaseous sulfuric acid concentrations are relatively similar ~~between~~in these
122 environments ([Chen et al., 2012](#); [Smith et al., 2008](#); [Wang et al., 2011b](#); [Zheng et al.,](#)
123 [2011](#)). Whether previous proxies developed for European and North American sites
124 work in Beijing remains to be tested. Furthermore, in addition to the gas phase reaction
125 between O(¹D) and water molecules (Crutzen and Zimmermann, 1991; Logan et al.,
126 1981), photolysis of HONO could be a potentially important source of OH radicals in
127 the atmosphere ~~not only~~ in the early morning (Alicke et al., 2002, 2003; Elshorbany et
128 al., 2009; Li et al., 2012) ~~and~~ ~~but also~~ during the daytime (Acker et al., 2005; Aumont
129 et al., 2003; Kleffmann, 2007). An experimental study measuring HONO near the
130 surface layer estimated that HONO was a main contributor to OH production in Beijing,
131 with HONO's contribution being larger than 70 % at around 12:00-13:00, except for
132 summer when the contribution of O₃ dominated (Hendrick et al., 2014). Given the
133 distinct characteristics of these two OH radical formation pathways, they both should
134 be included and evaluated separately when a proxy for atmospheric gaseous sulfuric
135 acid concentration is being built. The reactions between SO₂ and Ceriegee
136 intermediates formed from the ozonolysis of atmospheric alkenes could be a potential
137 source of sulfuric acid only in the absence of solar radiation (Boy et al., 2013; Mauldin
138 et al., 2012), so these reactions are expected to provide a minor contribution to the
139 formation of gaseous sulfuric acid during the daytime in urban Beijing.

140 In this study, gaseous sulfuric acid concentration was measured by a Long Time-
141 of-Flight Chemical Ionization Mass Spectrometer (LToF-CIMS) in February - March,
142 2018, in urban Beijing. A number of atmospheric parameters were recorded
143 concurrently, including the ultraviolet radiation B (UVB) intensity, concentrations of
144 O₃, NO_x, SO₂ and HONO, and particle number size distributions. The objective of this
145 study is to develop a robust daytime gaseous sulfuric acid concentration proxy for
146 Beijing, a representative Chinese megacity with urban atmospheric environments.

148 **2 Ambient measurements**

149 An intensive campaign was carried out from 9 February to 14 March, 2018 on the
150 fifth floor of a teaching building in the west campus of Beijing University of Chemical
151 Technology (39° 94' N, 116° 30' E). This monitoring site is 2 km to the west of the
152 West 3rd Ring Road and surrounded by commercial properties and residential dwellings.
153 Hence, this station can be regarded as a representative urban site.

154 The sulfuric acid concentration was measured by a LToF-CIMS (Aerodyne
 155 Research, Inc.) equipped with a nitrate chemical ionization source. Ambient air was
 156 drawn into the ionization source through a stainless-steel tube with a length of 1.6 m
 157 and a diameter of 3/4 inch. A mixture of a 3 standard cubic centimeter per minute (sccm)
 158 ultrahigh purity nitrogen flow containing nitric acid and a 20 standard liter per minute
 159 (slpm) pure air flow supplied by a zero-air generator (Aadco 737, USA), together as a
 160 sheath flow, was introduced into~~guided through~~ a PhotoIonizer (Model L9491,
 161 Hamamatsu, Japan) to produce nitrate reagent ions. This sheath flow was then
 162 introduced into a co-axial laminar flow reactor concentric to the sample flow. Nitrate
 163 ions were pushed to the middle of the sample flow under an electric field and
 164 subsequently charged sample molecules. For example, the atmospheric H₂SO₄
 165 molecules would be charged by nitrate reagent ion NO₃⁻(HNO₃)₀₋₂ and mainly produce
 166 HSO₄⁻ ions (m/z = 96.9601 Th), HSO₄⁻·HNO₃ ions (m/z = 159.9557 Th), and
 167 HSO₄⁻·(HNO₃)₂ ions (m/z = 222.9514 Th). In addition, HSO₄⁻·H₂SO₄ ions (m/z =
 168 194.9275 Th) were formed from ion-induced clustering of neutral sulfuric acid and
 169 bisulfate ions within the LToF-CIMS ion reaction zone, and also from the evaporation
 170 of dimethylamine (DMA) and the replacement of one molecule of H₂SO₄ with one
 171 bisulfate ion, HSO₄⁻, during the NO₃⁻ reagent ion charging of a stabilized neutral
 172 sulfuric acid dimer in the real atmosphere in presence of DMA or a molecule that works
 173 in the same way as DMA. During the campaign, the sample flow rate was kept at 8.8
 174 slpm, since mass flow controllers fixed the sheath flow rate and the excess flow rate,
 175 and the flow into the mass spectrometer (around 0.8 slpm) was fixed by the size of a
 176 pinhole between the ionization source and the mass spectrometer. The concentration of
 177 gaseous sulfuric acid was then determined by Eq. (2).

$$179 \quad [H_2SO_4] = \frac{HSO_4^- \cdot (HNO_3)_{0-2} + HSO_4^- \cdot H_2SO_4}{NO_3^- (HNO_3)_{0-2}} \cdot C \quad (2)$$

180
 181 where C is the calibration coefficient, and NO₃⁻(HNO₃)₀₋₂, HSO₄⁻·(HNO₃)₀₋₂ and
 182 HSO₄⁻·H₂SO₄ represent the signals of corresponding ions and are in units of counts per
 183 second (cps). The unit of resulting [H₂SO₄] is molecule cm⁻³. The CIMS was calibrated
 184 during the campaign with a home-made calibration box that can produce adjustable
 185 concentrations of gaseous sulfuric acid from SO₂ and OH radicals following the
 186 protocols in previous literatures (Kürten et al., 2012; Zheng et al., 2015). We obtain a
 187 calibration coefficient of 3.79×10^9 molecule cm⁻³ for our instrument and use $1.1 \times$

188 10^{10} molecule cm^{-3} as the effective calibration coefficient, after taking into account
 189 the diffusion losses in the stainless-steel tube and the nitrate chemical ionization
 190 source. During the campaign, the sample flow rate was kept at 8.4 slpm, since mass flow
 191 controllers fixed the sheath flow rate and the excess flow rate and the flow into the mass
 192 spectrometer (around 0.4 slpm) was fixed by the size of a pinhole between the
 193 ionization source and the mass spectrometer. The CIMS was calibrated twice during
 194 the campaign following the protocols in previous literatures (Kürten et al., 2012; Zheng
 195 et al., 2015). Here we use 1.1×10^{10} molecule cm^{-3} as the calibration coefficient, after
 196 taking into account diffusion losses in the stainless-steel tube and the nitrate chemical
 197 ionization source. The obtained mass spectra were analyzed with a tofTools package
 198 based on the MATLAB software (Junninen et al., 2010).

199 Ambient particle number size distributions down to about 1 nm were measured
 200 using a combination of a scanning mobility particle sizer spectrometer (SMPS)
 201 equipped with a diethylene glycol-based condensation particle counter (DEG-CPC, ~1-
 202 10 nm) and a conventional particle size distribution system (PSD, ~3 nm - 10 μm 3-700
 203 nm) consisting of a pair of aerosol mobility spectrometers developed by Tsinghua
 204 University (Cai et al., 2017; Jiang et al., 2011; Liu et al., 2016). The values of CS were
 205 calculated following Eq. (3) (Dal Maso et al., 2002):
 206

$$207 \quad CS = 2\pi D \int_0^{\infty} D_p \beta_m(D_p) n(D_p) dD_p = 2\pi D \sum_i \beta_i D_{pi} N_i \quad (3)$$

208 where D_{pi} is the geometric mean diameter of particles in the size bin i and N_i is the
 209 particle number concentration in the corresponding size bin. D is the diffusion
 210 coefficient of gaseous sulfuric acid, and β_m represents a transition-regime correction
 211 factor dependent on that could be defined as a function of the Knudsen number (Fuchs
 212 and Sutugin, 1971; Gopalakrishnan and Hogan Jr., 2011).
 213

214 SO_2 , O_3 and NO_x concentrations were measured using a SO_2 analyzer (Model 43i,
 215 Thermo, USA), a O_3 analyzer (Model 49i, Thermo, USA) and a NO_x analyzer (Model
 216 42i, Thermo, USA) with the detection limits of 0.1 ppbv, 0.5 ppbv and 0.4 ppbv,
 217 respectively. The above instruments were pre-calibrated before the campaign. The UVB
 218 (280 - 315 nm) intensity (UV-S-B-T, KIPP&ZONEN, The Netherlands) was measured
 219 on the rooftop of the building. Atmospheric HONO concentrations were measured by
 220 a home-made HONO analyzer with a detection limit of 0.01 ppbv (Tong et al., 2016).

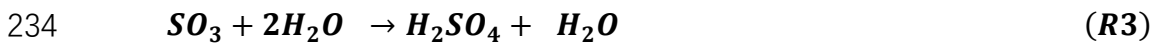
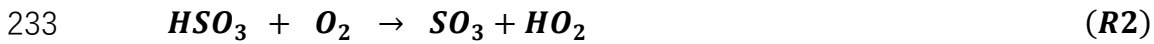
221 Particle number size distributions and concentrations of gaseous sulfuric acid, SO₂,
 222 O₃, NO_{x2} and HONO were recorded with a time resolution of 5 min, and the UVB
 223 intensity with time resolution of 1 min. A linear interpolation method was used for
 224 deriving the variables with the same time intervals, *i.e.*, 5 min. Only data between local
 225 sunrise and sunset were used in the subsequent analysis.

226

227 **3 Development of a proxy for atmospheric gaseous sulfuric acid**

228 We derived the gaseous sulfuric acid concentration proxy on the basis of currently
 229 accepted formation pathways of sulfuric acid in the atmosphere (R1-R3) (Finlayson-
 230 Pitts and Pitts, 2000; Stockwell and Calvert, 1983):

231



235

236 The reaction (R1) is the rate-limiting step of this formation pathway (Finlayson-Pitts
 237 and Pitts, 2000), so our proxy will consider the two major processes that determine the
 238 abundance of gaseous sulfuric acid: the formation of gaseous sulfuric acid from
 239 reactions between SO₂ and OH radicals, and the loss of gaseous sulfuric acid due to its
 240 condensation onto pre-existing particles (Dal Maso et al., 2002; Kulmala et al., 2012;
 241 Pirjola et al., 1999).

242 The rate of change of sulfuric acid concentration can be written as Eq. (4)
 243 (Mikkonen et al., 2011):

244

$$245 \quad d[\text{H}_2\text{SO}_4]/dt = k \cdot [\text{OH}] \cdot [\text{SO}_2] - [\text{H}_2\text{SO}_4] \cdot CS \quad (4)$$

246

247 where k is a temperature-dependent reaction constant given by Eq. (5) (DeMore et al.,
 248 1997; Mikkonen et al., 2011).

249

$$250 \quad k = \frac{A \cdot k_3}{(A + k_3)} \cdot \exp \left\{ k_5 \cdot \left[1 + \log_{10} \left(\frac{A}{k_3} \right)^{21-1} \right] \right\} \quad \text{cm}^3(\text{molecule} \cdot \text{s})^{-1} \quad (5)$$

251

252 where $A = k_1 \cdot [M] \cdot \left(\frac{300}{T}\right)^{k_2}$, $[M]$ represents the density of the air in molecule cm⁻³

253 ~~as calculated by~~ $0.101 \cdot (1.381 \cdot 10^{-23} \cdot T)^{-1}$, $k_1 = 4 \cdot 10^{-31}$, $k_2 = 3.3$, $k_3 = 2 \cdot$
 254 10^{-12} ~~and~~ $k_5 = -0.8$, where k is a temperature-dependent reaction constant (DeMore
 255 ~~et al., 1997).~~

256 To simplify the calculation, the production and loss of sulfuric acid can be assumed
 257 to be at pseudo steady-state (Mikkonen et al., 2011; Petäjä et al., 2009). Then the
 258 sulfuric acid concentration can be written as Eq. (6).

$$260 \quad [H_2SO_4] = k \cdot [OH] \cdot [SO_2] \cdot CS^{-1} \quad (6)$$

261
 262 Atmospheric OH radical measurements represent a major challenge as well. Since
 263 previous studies suggest that the OH radical concentration is strongly correlated with
 264 the intensity of UVB, [OH] could be replaced with UVB intensity in the proxy equation
 265 (Petäjä et al., 2009; Rohrer and Berresheim, 2006). Although photolysis of O₃
 266 ($\lambda < 320 \text{ nm}$) and subsequent reactions with H₂O are considered to be the dominant
 267 source of OH radicals in the atmosphere (Logan et al., 1981), recent studies argue that
 268 photolysis of HONO ($\lambda < 400 \text{ nm}$) is a potentially important OH radical formation
 269 pathway (Hendrick et al., 2014; Kleffmann, 2007; Su et al., 2011; Villena et al., 2011).
 270 Thus, we attempt to introduce both O₃ and HONO into the proxy equation and evaluate
 271 their effects on the concentration of OH radicals.

272 In practice, the ~~exponents for variables~~~~values of the exponential factors~~ in
 273 nonlinear fitting procedures are rarely equal to 1 (Mikkonen et al., 2011), so we
 274 replaced the factors x_i with $x_i^{w_i}$ in the proxy, where x_i can be an atmospheric
 275 variable ~~such as UVB and [SO₂]~~, and w_i defines x_i ' weight in the proxy. Since k is a
 276 temperature-dependent reaction constant and varies within a 10 % range (in the
 277 atmosphere temperature range of 267.6 - 292.6 K), ~~i.e., the actual atmospheric~~
 278 ~~temperature variation in this study, we approximately regard~~ k as a constant and use a
 279 ~~new scaling factor~~ k_0 . ~~This methodology has been used previously in the proxies of~~
 280 ~~gaseous sulfuric acid~~~~we further replaced~~ k with a scaling factor k_0 ~~that is also used in~~
 281 ~~the proxy methods built~~ in Hyytiä Southern Finland (Petäjä et al., 2009). As a result,
 282 the general proxy equation can be written as Eq. (7), with the UVB intensity, [SO₂],
 283 condensation sink (CS), [O₃], and [HONO] (or [NO_x]) as predictor variables:

$$285 \quad [H_2SO_4] = f(k_0, x_i^{w_i}), \quad x_i = UVB, [SO_2], CS, [O_3], [HONO] \dots \quad (7)$$

287 The nonlinear curve-fitting procedures using iterative least square estimation for
288 the proxies of gaseous sulfuric acid concentration based on Eq. (7) were performed by
289 a custom-made MATLAB software. In addition to the correlation coefficient (R),
290 relative error (RE) is used to evaluate the performance of proxies in the statistical
291 analysis and can be written as Eq. (8).

$$RE = \frac{1}{n} \cdot \sum_{i=1}^n \frac{|[H_2SO_4]_{proxy,i} - [H_2SO_4]_{meas,i}|}{[H_2SO_4]_{meas,i}} \quad (8)$$

294 4 Results and discussion

295 4.1 General Characteristics of daytime sulfuric acid and atmospheric parameters

296 Table 1 summarizes the mean, median and 5-95 % percentiles of gaseous sulfuric
297 acid concentrations and other variables measured during the daytime of the campaign.
298 The 5-95 % percentile ranges of the UVB intensity, [SO₂], [NO_{x2}] and [O₃] were 0-0.45
299 W m⁻², 0.9-11.4 ppbv, 3.3-61.4 ppbv and 3.5-23.3 ppbv, respectively. Compared with
300 the sites in the study by Mikkonen et al. (2011), Beijing was characterized with a factor
301 of 1.4-13.1 higher mean [SO₂] but a factor of 3.4-5.4 lower mean [O₃]. The 5-95 %
302 percentile range of CS in Beijing was 0.01-0.24 s⁻¹, which is about 10-100 times
303 higher~~1-2 orders of magnitude larger~~ than corresponding value ranges in Europe and
304 North America. The concentration of gaseous sulfuric acid during this campaign was
305 (2.2 – 10.0) × 10⁶ molecule cm⁻³ ~~was in the~~ 5-95 % percentile range ~~of~~, relatively
306 similar to observed elsewhere around the world. A diurnal mean concentration of 0.74
307 ppbv for HONO was observed in this campaign, consistent with previous long-term
308 HONO measurements of about 0.48-1.8 ppbv (averaged values) in winter in Beijing
309 (Hendrick et al., 2014; Spataro et al., 2013; Wang et al., 2017), which is a factor of 4-
310 10 higher than HONO concentrations measured in Europe (Alicke et al., 2002, 2003).
311 In addition, Beijing is dry in winter with a mean ambient relative humidity of 28 %
312 during the campaign.~~an ambient relative humidity generally lower than 60%.~~

313 4.2 Correlations between [H₂SO₄] and atmospheric variables

314 Table 2 summarizes the correlation coefficients between [H₂SO₄] and atmospheric
315 variables using a Spearman-type correlation analysis. ~~Note that only correlations with~~
316 ~~p-values smaller than 0.01 were included to ensure a statistical significance.~~ Clearly,
317 the UVB intensity is an isolated variable that is independent of all the other variables
318
319

320 but that imposes a positive influence on O₃ because of photochemical formation of
321 ozone, and a negative influence on HONO because of HONO's photochemical
322 degradation. The sulfuric acid concentration shows positive correlations with all the
323 other variables. The correlation coefficients between [H₂SO₄] and [SO₂] and between
324 [H₂SO₄] and UVB intensity are 0.74 and 0.46, respectively, which indicate that [SO₂]
325 and UVB have important influences on the formation of atmospheric gaseous sulfuric
326 acid, consistent with the accepted formation pathway of gaseous sulfuric acid from the
327 reaction between SO₂ and OH radicals. Accordingly, [O₃] and [HONO] show positive
328 correlations with [H₂SO₄] because both O₃ and HONO could be precursors of OH
329 radicals. Surprisingly, a high positive correlation coefficient (0.6) was found between
330 [H₂SO₄] and CS, which is in contrast to the conventional thought that CS describes the
331 loss of gaseous sulfuric acid molecules onto pre-existing particles and thus should show
332 a negative correlation. CS correlates well with [SO₂] ($r = 0.83$) and [NO_{x2}] ($r = 0.77$):
333 a high CS value, as an indicator of ~~an~~ atmospheric particle ~~_~~pollution, is thus usually
334 accompanied with a high concentration of both SO₂ and NO_{x2} in urban China,
335 indicating co-emissions. A strong correlation between [HONO] and [NO_{x2}] ($r = 0.88$)
336 in our measurement is supported by the fact that HONO can be either heterogeneously
337 formed by reactions of NO₂ on various surfaces (Calvert et al., 1994) or homogeneously
338 formed by the gas phase NO + OH reaction, between which the former likely dominate
339 for the daytime HONO production in urban Beijing (Liu et al., 2014).

340 Since the UVB intensity and [SO₂] have been reported as the dominating factors
341 for the formation of sulfuric acid (Mikkonen et al., 2011; Petäjä et al., 2009), we further
342 explored the relationship of the measured sulfuric acid concentrations with the UVB
343 intensity and [SO₂] using the nonlinear curve-fitting method with a single variable.
344 Figure 1a presents a scatter plot of [H₂SO₄] against the UVB intensity, color-coded by
345 [SO₂]. A good correlation layering with~~with a clear lamination by~~ [SO₂] is evident,
346 indicating that the UVB intensity and [SO₂] together play an important role in the
347 formation of sulfuric acid. A similar scatter plot (Figure 1b) of [H₂SO₄] against [SO₂],
348 color-coded by the UVB intensity, leads to a similar conclusion.

349

350 4.3 Proxy construction

351 Similar to the non-linear proxies suggested by Mikkonen et al. (2011), we tested a
352 number of proxies for gaseous sulfuric acid, listed in Table 3 with their respective fitting
353 parameters and performance summarized in Table 4. The scatter plots of observed

354 [H₂SO₄] *versus* predicted values given by proxies are presented in Fig. S1. In these
355 proxies, the concentration of a gaseous species is in the unit of molecule cm⁻³, the unit
356 of the UVB intensity is W m⁻², the unit of CS is s⁻¹, and k_0 is a scaling factor.

357 The proxy N1 was built by using the UVB intensity and [SO₂] as the source terms
358 and CS as the sink term, which follows the conventional idea of the H₂SO₄ formation
359 and loss in the atmosphere. CS was then removed from this proxy to examine the
360 performance of the proxy N2 that has~~ve~~ the UVB intensity and [SO₂] as the only
361 predictor variables. Since the formation of OH radicals in the atmosphere depends on
362 precursors in addition to UVB, we further attempted to introduce the OH precursor term
363 into the H₂SO₄ proxy. The proxies N3 and N4 were built by introducing O₃ as the only
364 OH precursor to evaluate its influence on the formation of sulfuric acid. Furthermore,
365 we added HONO as another potential precursor for OH radicals, resulting in the proxies
366 N5 and N6. Lastly, the proxy N7 was built by replacing [HONO] with [NO_{x2}] because
367 firstly, HONO is not regularly measured, and secondly, a good linear correlation
368 between [HONO] and [NO_{x2}] was generally observed in the daytime during this
369 campaign, although higher [HONO]/[NO_{x2}] ratios were observed in the morning due to
370 the accumulation of HONO during the night (Figure 2). RH was not considered in the
371 current study because a test by introducing RH into the proxies do not result in a
372 significantly better performance, which is consistent with those conclusions~~the~~
373 ~~introduction of RH into the proxy did not yield significantly better results~~ in the
374 Mikkonen et al. study (2011).

375 As shown in Table 4, the correlation coefficients are in the range of 0.83-0.86 and
376 ~~RMAEs~~ are in the range of ~~19.1-20.0 % (0.94 – 1.03) × 10⁶ molecule cm⁻³~~. The
377 exponents for the UVB intensity range from 0.13 to 0.16, and those for [SO₂] generally
378 range from 0.38 to 0.41, except in case of the proxy N6 (b=0.33). The obtained
379 exponent b for [SO₂] is significantly smaller than 1 unlike the assumptioned in Eq.
380 ~~(63)~~, mainly because [SO₂] is also an indicator of air pollution that usually influences
381 the sinks of both OH radicals and sulfuric acid. The exponent for [SO₂] ranged from
382 0.5 to 1.04 in the previous proxy study for European and North American sites
383 (Mikkonen et al., 2011), including values from 0.48 to 0.69 in Atlanta, GA, USA, which
384 was probably quite a polluted site because the measurements were conducted only 9
385 km away from a coal-fired power plant. The obtained value range of the exponent b
386 for [SO₂] in our study is probably related to the urban nature of Beijing. The value of
387 exponent c for CS in the proxy N1 is as low as 0.03, which either might be due to the

388 covariance of CS and certain H₂SO₄ sources that cancels the dependence on CS, or it
389 might indicate that CS is actually insufficient in regulating the H₂SO₄ concentration, as
390 recently suggested by Kulmala et al. (2017). By comparing the proxies N1 and N2, we
391 can see that CS plays a minor role because the exponents of [SO₂] and UVB, the overall
392 correlation coefficient and the RMAEs are almost identical with and without CS. We
393 can see the negligible role of CS also when comparing the results of the proxies N3 and
394 N4 where O₃ is considered. However, the role of CS becomes evident between the
395 proxies N5 and N6 when HONO is introduced: the exponents of [SO₂], [O₃], and
396 [HONO] significantly increased when taking into account the CS, suggesting that the
397 covariance between HONO and CS can explain, at least partially, the close-to-zero
398 exponent of CS in the proxies N1-N4. In addition, when [O₃] is introduced as the only
399 precursor for OH radicals, minor improvements in the correlation coefficient and
400 RMAE were obtained, as suggested by comparing the proxies N3 and N1. When both
401 [O₃] and [HONO] were introduced as OH precursors in the proxies N5-N7, REs have
402 noticeable improvements, and correlation coefficients improved slightly.~~MAE and~~
403 ~~correlation coefficient significantly improved.~~ Altogether, these observations suggest
404 that it is crucial to introduce HONO into the proxy, both in our study and also likely for
405 the previous work where the exponent of CS is close-to-zero (Mikkonen et al., 2011).

406 Although so far the proxy N5 had the best fitting quality, it is impractical to
407 explicitly include [HONO] because HONO measurements are very challenging. As
408 shown in Fig. 2, [HONO] and [NO_{x2}] ~~are~~ tended to correlate linearly with each other in
409 the daytime during this campaign, with a linearly fitted [HONO]/[NO_{x2}] ratio of around
410 0.03 and a relative error of 0.42~~mean absolute error (MAE) of 0.3 ppbv. Similar, strong~~
411 ~~linearity was observed in a previous study by Hao et al. (2006) who attributed this~~
412 ~~observation to the heterogeneous conversion of NO₂ to HONO. Only o~~Occasionally
413 ~~slightly~~ higher [HONO]/[NO_{x2}] ratios ~~in the morning~~ could be seen in the morning,
414 which might be due to the fact that HONO concentration could have an accumulation
415 process during the nighttime and lead to a deviation from the steady state. ~~deviation~~
416 ~~from the steady state. Bernard et al. (2016) reported that [NO₂] has a similar diurnal~~
417 ~~behavior to that of [HONO] and hence the ratio of [HONO]/[NO₂] varies slightly during~~
418 ~~the diurnal cycle.~~ Therefore, due to the good correlation, the proxy N7 replaces [HONO]
419 by [NO_{x2}], a more easily measured variable, and performs equally well with the proxy
420 N5.

421 Clearly, the proxy N2 provides the simplest parameterization, but the proxies N5

422 and N7 result in the best fitting quality because of the introduction of [HONO]. Figure
423 3 presents the RE values for the proxies N2 and N7, respectively, as a function of linear
424 bins of measured sulfuric acid concentrations. The performance of the proxy N7 is
425 considerably better than that of the proxy N2 in the sulfuric acid concentration range of
426 $(2.2 - 10) \times 10^6$ molecule cm^{-3} , which covers the 5-95% percentiles of sulfuric acid
427 concentration in this study. In the worst scenario, RE of proxy N2 is 1.2 times as high
428 as that of proxy N7, e.g., REs are 16.75 % and 13.99 %, respectively, in the sulfuric
429 acid concentration bin of $(4 - 5) \times 10^6$ molecule cm^{-3} , and 16.71 % and 14.42 %,
430 respectively, in the bin of $(7 - 8) \times 10^6$ molecule cm^{-3} .

431 432 **4.4 Comparison of measured and predicted [H₂SO₄]**

433 A comparison between measured and predicted [H₂SO₄] was performed. Figure 4
434 includes calculated results from the proxies N2 and N7 as well as from a proxy
435 constructed according to measurement in a boreal forest site, Finland, *i.e.*, Eq (1) (Petäjä
436 et al., 2009). The measured daytime [H₂SO₄] on 10 March, 2018, was above 4×10^6
437 molecules cm^{-3} when averaged to with a time resolution of 5 min. The predicted [H₂SO₄]
438 using the proxies N2 and N7 both track the measured [H₂SO₄] pretty well, even when
439 an unexpected dip in the sulfuric acid concentration was observed at around 10:00-
440 11:00. The performance of the proxy N7 is better than that of proxy N2 during the entire
441 day, consistent with our results in Fig. 3. The proxy by Petäjä et al. (2009)
442 underestimated the concentrations of sulfuric acid by a factor of 20 or so, which can be
443 attributed to the very different values of CS between Beijing and the boreal forest. The
444 fact that $[\text{H}_2\text{SO}_4]_{\text{Petäjä et al.}}$ does not track the measured [H₂SO₄] even after including
445 a scaling factor indicates that proxies are site-specific and do not necessarily work well
446 in locations other than where they have originally been developed for. In addition, the
447 direct performance comparison between the proxy N2 and the proxy by Petäjä et al.
448 (2009) indicates the importance of assigning exponential weights to variables in the
449 nonlinear fitting procedures, which is consistent with results by Mikkonen et al. (2011).

450 451 **5 Summary and conclusions**

452 Sulfuric acid is a key precursor for atmospheric new particle formation. In this
453 study, we constructed a number of proxies for gaseous sulfuric acid concentration
454 according to our measurements in urban Beijing during the winter. According to the
455 obtained proxies and their performance, the UVB intensity and [SO₂] were the

456 dominant influencing factors. Hence, the simplest proxy (Proxy N2) only involves
 457 UVB intensity and [SO₂] as shown by Eq. (9). The units of [H₂SO₄] and [SO₂] are
 458 molecule cm⁻³, and the unit of UVB is W m⁻².

$$459 \quad [H_2SO_4] = 280.05 \cdot UVB^{0.14} \cdot [SO_2]^{0.40} \quad (9)$$

461 ~~This proxy resulted in a relative deviation of up to 29 %.~~

463 For a comprehensive consideration of the formation pathways of OH radicals, For
 464 the best proxy accuracy, [O₃] and [HONO] as well as CS should be included (Proxy
 465 N5), as shown by Eq. (10). The units of [H₂SO₄], [SO₂], [O₃] and [HONO] are molecule
 466 cm⁻³, the unit of UVB is W m⁻², and the unit of CS is s⁻¹.

$$468 \quad [H_2SO_4] = 0.0072 \cdot UVB^{0.15} \cdot [SO_2]^{0.41} \cdot CS^{-0.17} \cdot ([O_3]^{0.36}$$

$$469 \quad + [HONO]^{0.38}) \quad (10)$$

471 Since HONO measurements are not a regular practice, we can further replace [HONO]
 472 with [NO_{x2}], shown in Eq. (11), which can be justified by the strong linear correlation
 473 between [HONO] and [NO_{x2}] observed in this study. The units of [H₂SO₄], [SO₂], [O₃]
 474 and [NO_x] are molecule cm⁻³, the unit of UVB is W m⁻², and the unit of CS is s⁻¹.

$$476 \quad [H_2SO_4] = 0.0013 \cdot UVB^{0.13} \cdot [SO_2]^{0.40} \cdot CS^{-0.17} \cdot ([O_3]^{0.44}$$

$$477 \quad + [NO_{x2}]^{0.41}) \quad (11)$$

479 We consider this last proxy more reasonable than the others due to the following reasons:
 480 first, it makes the equation physically meaningful as the CS starts to be involved as a
 481 sink term, and second, the ~~absolute and relative fitting error~~ RE was ~~ere~~ reduced
 482 considerably compared with the other proxies. Overall, this suggests that the photolysis
 483 of O₃ and HONO are both important OH sources in urban Beijing.

484 As a summary, we recommend using the simplest proxy (proxy N2 as shown in
 485 Eq. (9)) and a more accurate proxy (Proxy N7 as shown in Eq. (11)) for calculating
 486 daytime gaseous sulfuric acid concentrations in the urban Beijing atmosphere. It is clear
 487 that the current proxies are based on only a month-long campaign of sulfuric acid
 488 measurements in urban Beijing during winter. Given the dramatic reduction in the
 489 concentration of SO₂ in recent years (Wang et al., 2018) and the strong dependence of

490 calculated [H₂SO₄] on [SO₂], the performance of the proxies in the past and future years
491 remain to be evaluated. Furthermore, the proxies might be site-specific and season-
492 specific. Since the proxies were derived with atmospheric parameters in winter, in
493 urban Beijing, the exponents for atmospheric variables in the proxy could have different
494 values for other cities or other seasons. Thus, the proxies in this study should be further
495 tested before their application to other Chinese megacities or other
496 seasons.~~Nevertheless, our work here shows the importance of heterogeneous chemistry~~
497 ~~as a potential source of OH radicals in an urban air; however, the proxies might be site-~~
498 ~~specific and should be further tested before their application to other Chinese~~
499 ~~megacities.~~

500

501 **Author contributions**

502 LW designed this study. YL (Yiqun Lu), CY, YF, YC, YL (Yiliang Liu), GY, YW, YZ, RY, RB
503 and CD conducted the field campaign. YL (Yiqun Lu) analyzed data with contributions from
504 LW and all the other co-authors. YL (Yiqun Lu) and LW wrote the manuscript with
505 contributions from all the other co-authors.

506

507 **Acknowledgement**

508 This study was financially supported by the National Key R&D Program of China
509 (2017YFC0209505), and the National Natural Science Foundation of China (41575113,
510 91644213).

511 **References**

- 512 Acker, K., Möller, D., Auel, R., Wieprecht, W. and Kalaß, D.: Concentrations of nitrous acid, nitric
513 acid, nitrite and nitrate in the gas and aerosol phase at a site in the emission zone during
514 ESCOMPTE 2001 experiment, *Atmos. Res.*, 74(1–4), 507–524,
515 doi:10.1016/j.atmosres.2004.04.009, 2005.
- 516 Alicke, B., Platt, U. and Stutz, J.: Impact of nitrous acid photolysis on the total hydroxyl radical
517 budget during the Limitation of Oxidant Production/Pianura Padana Produzione di Ozono
518 study in Milan, *J. Geophys. Res. Atmos.*, 107(22), doi:10.1029/2000JD000075, 2002.
- 519 Alicke, B., Geyer, A., Hofzumahaus, A., Holland, F., Konrad, S., Patz, H. W., Schafer, J., Stutz, J.,
520 Volz-Thomas, A. and Platt, U.: OH formation by HONO photolysis during the BERLIOZ
521 experiment, *J. Geophys. Res.*, 108(D4), 8247, doi:10.1029/2001JD000579, 2003.
- 522 Almeida, J., Schobesberger, S., Kürten, A., Ortega, I. K., Kupiainen-Määttä O., Praplan, A. P.,
523 Adamov, A., Amorim, A., Bianchi, F., Breitenlechner, M., David, A., Dommen, J., Donahue,
524 N. M., Downard, A., Dunne, E., Duplissy, J., Ehrhart, S., Flagan, R. C., Franchin, A., Guida,
525 R., Hakala, J., Hansel, A., Heinritzi, M., Henschel, H., Jokinen, T., Junninen, H., Kajos, M.,
526 Kangasluoma, J., Keskinen, H., Kupc, A., Kurtén, T., Kvashin, A. N., Laaksonen, A., Lehtipalo,
527 K., Leiminger, M., Leppä J., Loukonen, V., Makhmutov, V., Mathot, S., McGrath, M. J.,
528 Nieminen, T., Olenius, T., Onnela, A., Petäjä T., Riccobono, F., Riipinen, I., Rissanen, M.,
529 Rondo, L., Ruuskanen, T., Santos, F. D., Sarnela, N., Schallhart, S., Schnitzhofer, R., Seinfeld,
530 J. H., Simon, M., Sipilä M., Stozhkov, Y., Stratmann, F., Tomé A., Tröstl, J., Tsagkogeorgas,
531 G., Vaattovaara, P., Viisanen, Y., Virtanen, A., Vrtala, A., Wagner, P. E., Weingartner, E.,
532 Wex, H., Williamson, C., Wimmer, D., Ye, P., Yli-Juuti, T., Carslaw, K. S., Kulmala, M.,
533 Curtius, J., Baltensperger, U., Worsnop, D. R., Vehkamäki, H. and Kirkby, J.: Molecular
534 understanding of sulphuric acid-amine particle nucleation in the atmosphere, *Nature*,
535 502(7471), 359–363, doi:10.1038/nature12663, 2013.
- 536 Arnold, F. and Fabian, R.: First measurements of gas phase sulphuric acid in the stratosphere, *Nature*,
537 283(3), 55–57, 1980.
- 538 Aumont, B., Chervier, F. and Laval, S.: Contribution of HONO sources to the NO_x/HO_x/O₃
539 chemistry in the polluted boundary layer, *Atmos. Environ.*, 37(4), 487–498,
540 doi:10.1016/S1352-2310(02)00920-2, 2003.
- 541 Benson, D. R., Young, L. H., Kameel, F. R. and Lee, S. H.: Laboratory-measured nucleation rates
542 of sulfuric acid and water binary homogeneous nucleation from the SO₂ + OH reaction,
543 *Geophys. Res. Lett.*, 35(11), 1–6, doi:10.1029/2008GL033387, 2008.
- 544 Berresheim, H., Elste, T., Plass-Dülmer, C., Eisele, F. L. and Tanner, D. J.: Chemical ionization
545 mass spectrometer for long-term measurements of atmospheric OH and H₂SO₄, *Int. J. Mass*
546 *Spectrom.*, 202(1–3), 91–109, doi:10.1016/S1387-3806(00)00233-5, 2000.
- 547 Bianchi, F., Tröstl, J., Junninen, H., Frege, C., Henne, S., Hoyle, C. R., Molteni, U., Herrmann, E.,
548 Adamov, A., Bukowiecki, N., Chen, X., Duplissy, J., Gysel, M., Hutterli, M., Kangasluoma,
549 J., Kontkanen, J., Kurten, A., Manninen, H. E., Munch, S., Peräkylä O., Petäjä T., Rondo, L.,
550 Williamson, C., Weingartner, E., Curtius, J., Worsnop, D. R., Kulmala, M., Dommen, J. and
551 Baltensperger, U.: New particle formation in the free troposphere: A question of chemistry and
552 timing, *Science*, 352(6289), 1109–1112, doi:10.1126/science.aad5456, 2016.

553 Boy, M., Mogensen, D., Smolander, S., Zhou, L., Nieminen, T., Paasonen, P., Plass-Dülmer, C.,
554 Sipilä M., Petäjä T., Mauldin, L., Berresheim, H. and Kulmala, M.: Oxidation of SO₂ by
555 stabilized Criegee intermediate (sCI) radicals as a crucial source for atmospheric sulfuric acid
556 concentrations, *Atmos. Chem. Phys.*, 13(7), 3865–3879, doi:10.5194/acp-13-3865-2013, 2013.

557 Cai, R., Chen, D. R., Hao, J. and Jiang, J.: A miniature cylindrical differential mobility analyzer for
558 sub-3 nm particle sizing, *J. Aerosol Sci.*, 106(September 2016), 111–119,
559 doi:10.1016/j.jaerosci.2017.01.004, 2017.

560 Calvert, J. G., Yarwood, G. and Dunker, A. M.: An evaluation of the mechanism of nitrous acid
561 formation in the urban atmosphere, *Res. Chem. Intermed.*, 20(3–5), 463–502,
562 doi:10.1163/156856794X00423, 1994.

563 Chen, M., Titcombe, M., Jiang, J., Jen, C., Kuang, C., Fischer, M. L. and Eisele, F. L.: Acid-base
564 chemical reaction model for nucleation rates in the polluted atmospheric boundary layer, *Proc.*
565 *Natl. Acad. Sci.*, 109(46), 18713–18718, doi:10.1073/pnas.1210285109, 2012.

566 Crutzen, P. J. and Zimmermann, P. H.: The changing photochemistry of the troposphere, *Tellus*,
567 43AB(December), 136–151, doi:10.3402/tellusb.v43i4.15397, 1991.

568 Dal Maso, M., Kulmala, M., Lehtinen, K. E. J., Mäkelä J. M., Aalto, P. and O’Dowd, C. D.:
569 Condensation and coagulation sinks and formation of nucleation mode particles in coastal and
570 boreal forest boundary layers, *J. Geophys. Res. Atmos.*, 107(19), doi:10.1029/2001JD001053,
571 2002.

572 DeMore, W. B., Sander, S. P., Golden, D. M., Hampson, R. F., Kurylo, M. J., Howard, C. J.,
573 Ravishankara, A. R., Kolb, C. E. and Molina, M. J.: Chemical kinetics and photochemical data
574 for use in stratospheric modeling, *JPL Publ.*, 97–4(12), 278, doi:10.1002/kin.550171010, 1997.

575 Dunn, M. J., Baumgardner, D., Castro, T., Mcmurry, P. H. and Smith, J. N.: Measurements of
576 Mexico City nanoparticle size distributions: Observations of new particle formation and
577 growth, *Geophys. Res. Lett.*, 31, L10102, doi:10.1029/2004GL019483, 2004.

578 Duplissy, J., Merikanto, J., Franchin, A., Tsagkogeorgas, G., Kangasluoma, J., Wimmer, D.,
579 Vuollekoski, H., Schobesberger, S., Lehtipalo, K., Flagan, R. C., Brus, D., Donahue, N. M.,
580 Vehkamäki, H., Almeida, J., Amorim, A., Barmet, P., Bianchi, F., Breitenlechner, M., Dunne,
581 E. M., Guida, R., Henschel, H., Junninen, H., Kirkby, J., Kürten, A., Kupc, A., Määttä, A.,
582 Makhmutov, V., Mathot, S., Nieminen, T., Onnela, A., Praplan, A. P., Riccobono, F., Rondo,
583 L., Steiner, G., Tome, A., Walther, H., Baltensperger, U., Carslaw, K. S., Dommen, J., Hansel,
584 A., Petäjä T., Sipilä M., Stratmann, F., Vrtala, A., Wagner, P. E., Worsnop, D. R., Curtius, J.
585 and Kulmala, M.: Effect of dimethylamine on the gas phase sulfuric acid concentration
586 measured by Chemical Ionization Mass Spectrometry, *J. Geophys. Res. Atmos.*, 1752–1775,
587 doi:10.1002/2015JD023538.Effect, 2016.

588 Eisele, F. L. and Tanner, D. J.: Measurement of the gas phase concentration of H₂SO₄ and methane
589 sulfonic acid and estimates of H₂SO₄ production and loss in the atmosphere, *J. Geophys. Res.*
590 *Atmos.*, 98(D5), 9001–9010, doi:10.1029/93JD00031, 1993.

591 Elshorbany, Y. F., Kurtenbach, R., Wiesen, P., Lissi, E., Rubio, M., Villena, G., Gramsch, E.,
592 Rickard, A. R., Pilling, M. J. and Kleffmann, J.: Oxidation capacity of the city air of Santiago,
593 Chile, *Atmos. Chem. Phys.*, doi:10.5194/acp-9-2257-2009, 2009.

594 Finlayson-Pitts, B. J. and Pitts, J. N.: Acid Deposition: Formation and Fates of Inorganic and

595 Organic Acids in the Troposphere, in *Chemistry of the Upper and Lower Atmosphere: Theory,*
596 *Experiments, and Applications*, p. 969, Academic Press, San Diego., 2000.

597 Fuchs, N. A. and Sutugin, A. G.: Highly dispersed aerosols, in *Topics in Current Aerosol Research*,
598 edited by G. M. HIDY and J. R. BROCK, p. 1, Pergamon., 1971.

599 Gopalakrishnan, R. and Hogan Jr., C. J.: Determination of the Transition Regime Collision Kernel
600 from Mean First Passage Times Determination of the Transition Regime Collision Kernel from
601 Mean First Passage Times, *Aerosol Sci. Technol.* ISSN, 45, 1499–1509,
602 doi:10.1080/02786826.2011.601775, 2011.

603 Hendrick, F., Cléner, K., Wang, P., De Mazière, M., Fayt, C., Gielen, C., Hermans, C., Ma, J. Z.,
604 Pinardi, G., Stavrou, T., Vlemmix, T. and Van Roozendaal, M.: Four years of ground-based
605 MAX-DOAS observations of HONO and NO₂ in the Beijing area, *Atmos. Chem. Phys.*, 14(2),
606 765–781, doi:10.5194/acp-14-765-2014, 2014.

607 Herrmann, E., Ding, A. J., Kerminen, V. M., Petäjä T., Yang, X. Q., Sun, J. N., Qi, X. M., Manninen,
608 H., Hakala, J., Nieminen, T., Aalto, P. P., Kulmala, M. and Fu, C. B.: Aerosols and nucleation
609 in eastern China: First insights from the new SORPES-NJU station, *Atmos. Chem. Phys.*, 14(4),
610 2169–2183, doi:10.5194/acp-14-2169-2014, 2014.

611 Jen, C. N., McMurry, P. H. and Hanson, D. R.: Stabilization of sulfuric acid dimers by ammonia,
612 methylamine, dimethylamine, and trimethylamine, *J. Geophys. Res. Atmos.*, 7502–7514,
613 doi:10.1002/2014JD021592.Received, 2014.

614 Jiang, J., Zhao, J., Chen, M., Eisele, F. L., Scheckman, J., Williams, B. J., Kuang, C. and McMurry,
615 P. H.: First measurements of neutral atmospheric cluster and 1-2 nm particle number size
616 distributions during nucleation events, *Aerosol Sci. Technol.*, 45(4),
617 doi:10.1080/02786826.2010.546817, 2011.

618 Jokinen, T., Sipilä M., Junninen, H., Ehn, M., Lönn, G., Hakala, J., Petäjä T., Mauldin, R. L.,
619 Kulmala, M. and Worsnop, D. R.: Atmospheric sulphuric acid and neutral cluster
620 measurements using CI-API-TOF, *Atmos. Chem. Phys.*, 12(9), 4117–4125, doi:10.5194/acp-
621 12-4117-2012, 2012.

622 Junninen, H., Ehn, M., Petäjä Luosujärvi, L., Kotiaho, T., Kostianen, R., Rohner, U., Gonin, M.,
623 Fuhrer, K., Kulmala, M. and Worsnop, D. R.: A high-resolution mass spectrometer to measure
624 atmospheric ion composition, *Atmos. Meas. Tech.*, 3(4), 1039–1053, doi:10.5194/amt-3-1039-
625 2010, 2010.

626 Kerminen, V.: Atmospheric new particle formation and growth : review of field observations,
627 *Environ. Res. Lett.*, 13, 103003, 2018.

628 Kerminen, V. M., Petäjä T., Manninen, H. E., Paasonen, P., Nieminen, T., Sipilä M., Junninen, H.,
629 Ehn, M., Gagné S., Laakso, L., Riipinen, I., Vehkamäki, H., Kurtén, T., Ortega, I. K., Dal
630 Maso, M., Brus, D., Hyvärinen, A., Lihavainen, H., Leppä J., Lehtinen, K. E. J., Mirme, A.,
631 Mirme, S., Hõrrak, U., Berndt, T., Stratmann, F., Birmili, W., Wiedensohler, A., Metzger, A.,
632 Dommen, J., Baltensperger, U., Kiendler-Scharr, A., Mentel, T. F., Wildt, J., Winkler, P. M.,
633 Wagner, P. E., Petzold, A., Minikin, A., Plass-Dülmer, C., Pöschl, U., Laaksonen, A. and
634 Kulmala, M.: Atmospheric nucleation: Highlights of the EUCAARI project and future
635 directions, *Atmos. Chem. Phys.*, 10(22), 10829–10848, doi:10.5194/acp-10-10829-2010, 2010.

636 Kirkby, J., Curtius, J., Almeida, J., Dunne, E., Duplissy, J., Ehrhart, S., Franchin, A., Gagné S.,

637 Ickes, L., Kürten, A., Kupc, A., Metzger, A., Riccobono, F., Rondo, L., Schobesberger, S.,
638 Tsagkogeorgas, G., Wimmer, D., Amorim, A., Bianchi, F., Breitenlechner, M., David, A.,
639 Dommen, J., Downard, A., Ehn, M., Flagan, R. C., Haider, S., Hansel, A., Hauser, D., Jud, W.,
640 Junninen, H., Kreissl, F., Kvashin, A., Laaksonen, A., Lehtipalo, K., Lima, J., Lovejoy, E. R.,
641 Makhmutov, V., Mathot, S., Mikkilä J., Minginette, P., Mogo, S., Nieminen, T., Onnela, A.,
642 Pereira, P., Petäjä T., Schnitzhofer, R., Seinfeld, J. H., Sipilä M., Stozhkov, Y., Stratmann, F.,
643 Tomé A., Vanhanen, J., Viisanen, Y., Vrtala, A., Wagner, P. E., Walther, H., Weingartner, E.,
644 Wex, H., Winkler, P. M., Carslaw, K. S., Worsnop, D. R., Baltensperger, U. and Kulmala, M.:
645 Role of sulphuric acid, ammonia and galactic cosmic rays in atmospheric aerosol nucleation,
646 *Nature*, 476, 429 [online] Available from: <http://dx.doi.org/10.1038/nature10343>, 2011.

647 Kleffmann, J.: Daytime sources of nitrous acid (HONO) in the atmospheric boundary layer,
648 *ChemPhysChem*, 8(8), 1137–1144, doi:10.1002/cphc.200700016, 2007.

649 Korhonen, P., Kulmala, M., Laaksonen, A., Viisanen, Y., McGraw, R. and Seinfeld, J. H.: Ternary
650 nucleation of H₂SO₄, NH₃, and H₂O in the atmosphere, *J. Geophys. Res.*,
651 doi:10.1029/1999JD900784, 1999.

652 Kuang, C., McMurry, P. H., McCormick, A. V. and Eisele, F. L.: Dependence of nucleation rates
653 on sulfuric acid vapor concentration in diverse atmospheric locations, *J. Geophys. Res. Atmos.*,
654 113(10), 1–9, doi:10.1029/2007JD009253, 2008.

655 Kuang, C., Chen, M., Zhao, J., Smith, J., McMurry, P. H. and Wang, J.: Size and time-resolved
656 growth rate measurements of 1 to 5nm freshly formed atmospheric nuclei, *Atmos. Chem. Phys.*,
657 12, 3573–3589, doi:10.5194/acp-12-3573-2012, 2012.

658 Kulmala, M. and Kerminen, V. M.: On the formation and growth of atmospheric nanoparticles,
659 *Atmos. Res.*, 90(2–4), 132–150, doi:10.1016/j.atmosres.2008.01.005, 2008.

660 Kulmala, M., Petäjä T., Nieminen, T., Sipilä M., Manninen, H. E., Lehtipalo, K., Dal Maso, M.,
661 Aalto, P. P., Junninen, H., Paasonen, P., Riipinen, I., Lehtinen, K. E. J., Laaksonen, A. and
662 Kerminen, V.-M.: Measurement of the nucleation of atmospheric aerosol particles, *Nat. Protoc.*,
663 7(9), 1651–1667, doi:10.1038/nprot.2012.091, 2012.

664 Kulmala, M., Kontkanen, J., Junninen, H., Lehtipalo, K., Manninen, H. E., Nieminen, T., Petäjä T.,
665 Sipilä M., Schobesberger, S., Rantala, P., Franchin, A., Jokinen, T., Järvinen, E., Äijälä M.,
666 Kangasluoma, J., Hakala, J., Aalto, P. P., Paasonen, P., Mikkilä J., Vanhanen, J., Aalto, J.,
667 Hakola, H., Makkonen, U., Ruuskanen, T., Mauldin, R. L., Duplissy, J., Vehkamäki, H., Bäck,
668 J., Kortelainen, A., Riipinen, I., Kurtén, T., Johnston, M. V., Smith, J. N., Ehn, M., Mentel, T.
669 F., Lehtinen, K. E. J., Laaksonen, A., Kerminen, V. M. and Worsnop, D. R.: Direct
670 observations of atmospheric aerosol nucleation, *Science*, 339(6122), 943–946,
671 doi:10.1126/science.1227385, 2013.

672 Kulmala, M., Kerminen, V.-M., Petäjä T., Ding, A. J. and Wang, L.: Atmospheric gas-to-particle
673 conversion: why NPF events are observed in megacities?, *Faraday Discuss.*, 200(0), 271–288,
674 doi:10.1039/C6FD00257A, 2017.

675 Kürten, A., Rondo, L., Ehrhart, S. and Curtius, J.: Calibration of a chemical ionization mass
676 spectrometer for the measurement of gaseous sulfuric acid, *J. Phys. Chem. A*, 116(24), 6375–
677 6386, doi:10.1021/jp212123n, 2012.

678 Kürten, A., Jokinen, T., Simon, M., Sipilä M., Sarnela, N., Junninen, H., Adamov, A., Almeida, J.,

679 Amorim, A., Bianchi, F., Breitenlechner, M., Dommen, J., Donahue, N. M., Duplissy, J.,
680 Ehrhart, S., Flagan, R. C., Franchin, A., Hakala, J., Hansel, A., Heinritzi, M., Hutterli, M.,
681 Kangasluoma, J., Kirkby, J., Laaksonen, A., Lehtipalo, K., Leiminger, M., Makhmutov, V.,
682 Mathot, S., Onnela, A., Petäjä T., Praplan, A. P., Riccobono, F., Rissanen, M. P., Rondo, L.,
683 Schobesberger, S., Seinfeld, J. H., Steiner, G., Tomé A., Tröstl, J., Winkler, P. M., Williamson,
684 C., Wimmer, D., Ye, P., Baltensperger, U., Carslaw, K. S., Kulmala, M., Worsnop, D. R. and
685 Curtius, J.: Neutral molecular cluster formation of sulfuric acid-dimethylamine observed in
686 real time under atmospheric conditions, *Proc. Natl. Acad. Sci.*, 111(42), 15019–15024,
687 doi:10.1073/pnas.1404853111, 2014.

688 Kürten, A., Münch, S., Rondo, L., Bianchi, F., Duplissy, J., Jokinen, T., Junninen, H., Sarnela, N.,
689 Schobesberger, S., Simon, M., Sipilä M., Almeida, J., Amorim, A., Dommen, J., Donahue, N.
690 M., Dunne, E. M., Flagan, R. C., Franchin, A., Kirkby, J., Kupc, A., Makhmutov, V., Petäjä
691 T., Praplan, A. P., Riccobono, F., Steiner, G., Tomé A., Tsagkogeorgas, G., Wagner, P. E.,
692 Wimmer, D., Baltensperger, U., Kulmala, M., Worsnop, D. R. and Curtius, J.:
693 Thermodynamics of the formation of sulfuric acid dimers in the binary (H₂SO₄-H₂O) and
694 ternary (H₂SO₄-H₂O-NH₃) system, *Atmos. Chem. Phys.*, 15(18), 10701–10721,
695 doi:10.5194/acp-15-10701-2015, 2015.

696 Kurtán, T., Petäjä T., Smith, J., Ortega, I. K., Sipilä M., Junninen, H., Ehn, M., Vehkamäki, H.,
697 Mauldin, L., Worsnop, D. R. and Kulmala, M.: The effect of H₂SO₄-amine clustering on
698 chemical ionization mass spectrometry (CIMS) measurements of gas-phase sulfuric acid,
699 *Atmos. Chem. Phys.*, 11(6), 3007–3019, doi:10.5194/acp-11-3007-2011, 2011.

700 Li, X., Brauers, T., Häsel, R., Bohn, B., Fuchs, H., Hofzumahaus, A., Holland, F., Lou, S., Lu, K.
701 D., Rohrer, F., Hu, M., Zeng, L. M., Zhang, Y. H., Garland, R. M., Su, H., Nowak, A.,
702 Wiedensohler, A., Takegawa, N., Shao, M. and Wahner, A.: Exploring the atmospheric
703 chemistry of nitrous acid (HONO) at a rural site in Southern China, *Atmos. Chem. Phys.*, 12(3),
704 1497–1513, doi:10.5194/acp-12-1497-2012, 2012.

705 Liu, J., Jiang, J., Zhang, Q., Deng, J. and Hao, J.: A spectrometer for measuring particle size
706 distributions in the range of 3 nm to 10 µm, *Front. Environ. Sci. Eng.*, 10(1), 63–72,
707 doi:10.1007/s11783-014-0754-x, 2016.

708 Liu, Z., Wang, Y., Costabile, F., Amoroso, A., Zhao, C., Huey, L. G., Stickel, R., Liao, J. and Zhu,
709 T.: Evidence of Aerosols as a Media for Rapid Daytime HONO Production over China,
710 *Environ. Sci. Technol.*, 48(24), 14386–14391, doi:10.1021/es504163z, 2014.

711 Logan, J. A., Prather, M. J., Wofsy, S. C. and Mcelroy, M. B.: Tropospheric chemistry: A global
712 perspective, *J. Geophys. Res.*, 86(C8), 7210–7254, doi:10.1029/JC086iC08p07210, 1981.

713 Mauldin, R. L., Berndt, T., Sipilä M., Paasonen, P., Petäjä T., Kim, S., Kurtán, T., Stratmann, F.,
714 Kerminen, V. M. and Kulmala, M.: A new atmospherically relevant oxidant of sulphur dioxide,
715 *Nature*, 488(7410), 193–196, doi:10.1038/nature11278, 2012.

716 Mikkonen, S., Romakkaniemi, S., Smith, J. N., Korhonen, H., Petäjä T., Plass-Duelmer, C., Boy,
717 M., McMurry, P. H., Lehtinen, K. E. J., Joutsensaari, J., Hamed, A., Mauldin, R. L., Birmili,
718 W., Spindler, G., Arnold, F., Kulmala, M. and Laaksonen, A.: A statistical proxy for sulphuric
719 acid concentration, *Atmos. Chem. Phys.*, 11(21), 11319–11334, doi:10.5194/acp-11-11319-
720 2011, 2011.

721 Nieminen, T., Lehtinen, K. E. J. and Kulmala, M.: Sub-10 nm particle growth by vapor
722 condensation-effects of vapor molecule size and particle thermal speed, *Atmos. Chem. Phys.*,
723 10(20), 9773–9779, doi:10.5194/acp-10-9773-2010, 2010.

724 Paasonen, P., Nieminen, T., Asmi, E., Manninen, H. E., Petäjä T., Plass-Dülmer, C., Flentje, H.,
725 Birmili, W., Wiedensohler, A., Hõrrak, U., Metzger, A., Hamed, A., Laaksonen, A., Facchini,
726 M. C., Kerminen, V. M. and Kulmala, M.: On the roles of sulphuric acid and low-volatility
727 organic vapours in the initial steps of atmospheric new particle formation, *Atmos. Chem. Phys.*,
728 10(22), 11223–11242, doi:10.5194/acp-10-11223-2010, 2010.

729 Petäjä T., Mauldin, R. L., Kosciuch, E., McGrath, J., Nieminen, T., Paasonen, P., Boy, M., Adamov,
730 A., Kotiaho, T. and Kulmala, M.: Sulfuric acid and OH concentrations in a boreal forest site,
731 *Atmos. Chem. Phys.*, 9(19), 7435–7448, doi:10.5194/acp-9-7435-2009, 2009.

732 Petäjä T., Sipilä M., Paasonen, P., Nieminen, T., Kurtén, T., Ortega, I. K., Stratmann, F.,
733 Vehkamäki, H., Berndt, T. and Kulmala, M.: Experimental observation of strongly bound
734 dimers of sulfuric acid: Application to nucleation in the atmosphere, *Phys. Rev. Lett.*, 106(22),
735 1–4, doi:10.1103/PhysRevLett.106.228302, 2011.

736 Pirjola, L., Kulmala, M., Wilck, M., Bischoff, A., Stratmann, F. and Otto, E.: Formation of sulphuric
737 acid aerosols and cloud condensation nuclei: An expression for significant nucleation and
738 model comparison, *J. Aerosol Sci.*, doi:10.1016/S0021-8502(98)00776-9, 1999.

739 Rohrer, F. and Berresheim, H.: Strong correlation between levels of tropospheric hydroxyl radicals
740 and solar ultraviolet radiation, *Nature*, 442(7099), 184–187, doi:10.1038/nature04924, 2006.

741 Sipilä M., Berndt, T., Petäjä T., Brus, D., Vanhanen, J., Stratmann, F., Patokoski, J., Mauldin, R.
742 L., Hyvärinen, A. P., Lihavainen, H. and Kulmala, M.: The role of sulfuric acid in atmospheric
743 nucleation, *Science*, 327(5970), 1243–1246, doi:10.1126/science.1180315, 2010.

744 Smith, J. N., Dunn, M. J., Vanreken, T. M., Iida, K., Stolzenburg, M. R., McMurry, P. H. and Huey,
745 L. G.: Chemical composition of atmospheric nanoparticles formed from nucleation in
746 Tecamac, Mexico: Evidence for an important role for organic species in nanoparticle growth,
747 *Geophys. Res. Lett.*, 35, L04808, doi:10.1029/2007GL032523, 2008.

748 Spataro, F., Ianniello, A., Esposito, G., Allegrini, I., Zhu, T. and Hu, M.: Occurrence of atmospheric
749 nitrous acid in the urban area of Beijing (China), *Sci. Total Environ.*, 447, 210–224,
750 doi:10.1016/j.scitotenv.2012.12.065, 2013.

751 Stockwell, W. R. and Calvert, J. G.: The mechanism of the HO-SO₂ reaction, *Atmos. Environ.*,
752 17(11), 2231–2235, doi:10.1016/0004-6981(83)90220-2, 1983.

753 Su, H., Cheng, Y., Oswald, R., Behrendt, T., Trebs, I., Meixner, F. X., Andreae, M. O., Cheng, P.,
754 Zhang, Y. and Pöschl, U.: Soil nitrite as a source of atmospheric HONO and OH radicals,
755 *Science*, 333(6049), 1616–1618, doi:10.1126/science.1207687, 2011.

756 Tong, S., Hou, S., Zhang, Y., Chu, B., Liu, Y., He, H., Zhao, P. and Ge, M.: Exploring the nitrous
757 acid (HONO) formation mechanism in winter Beijing: Direct emissions and heterogeneous
758 production in urban and suburban areas, *Faraday Discuss.*, 189, 213–230,
759 doi:10.1039/c5fd00163c, 2016.

760 Villena, G., Wiesen, P., Cantrell, C. A., Flocke, F., Fried, A., Hall, S. R., Hornbrook, R. S., Knapp,
761 D., Kosciuch, E., Mauldin, R. L., McGrath, J. A., Montzka, D., Richter, D., Ullmann, K.,
762 Walega, J., Weibring, P., Weinheimer, A., Staebler, R. M., Liao, J., Huey, L. G. and Kleffmann,

763 J.: Nitrous acid (HONO) during polar spring in Barrow, Alaska: A net source of OH radicals?,
764 J. Geophys. Res. Atmos., 116(24), 1–12, doi:10.1029/2011JD016643, 2011.

765 Wang, J., Zhang, X., Guo, J., Wang, Z. and Zhang, M.: Observation of nitrous acid (HONO) in
766 Beijing, China: Seasonal variation, nocturnal formation and daytime budget, Sci. Total
767 Environ., 587–588, 350–359, doi:10.1016/j.scitotenv.2017.02.159, 2017.

768 Wang, M., Zhu, T., Zhang, J. P., Zhang, Q. H., Lin, W. W., Li, Y. and Wang, Z. F.: Using a mobile
769 laboratory to characterize the distribution and transport of sulfur dioxide in and around Beijing,
770 Atmos. Chem. Phys., 11(22), 11631–11645, doi:10.5194/acp-11-11631-2011, 2011a.

771 Wang, Z., Zheng, F., Zhang, W. and Wang, S.: Analysis of SO₂ Pollution Changes of Beijing-
772 Tianjin-Hebei Region over China Based on OMI Observations from 2006 to 2017, Adv.
773 Meteorol., 2018, Article ID 8746068, 2018.

774 Wang, Z. B., Hu, M., Yue, D. L., Zheng, J., Zhang, R. Y., Wiedensohler, A., Wu, Z. J., Nieminen,
775 T. and Boy, M.: Evaluation on the role of sulfuric acid in the mechanisms of new particle
776 formation for Beijing case, Atmos. Chem. Phys., 11(24), 12663–12671, doi:10.5194/acp-11-
777 12663-2011, 2011b.

778 Weber, R. J., Marti, J. J., McMurry, P. H., Eisele, F. L., Tanner, D. J. and Jefferson, a.:
779 Measurements of new particle formation and ultrafine particle growth rates at a clean
780 continental site, J. Geophys. Res. Atmos., 102, 4375–4385, doi:10.1029/96JD03656, 1997.

781 Wu, F., Xie, P., Li, A., Mou, F., Chen, H., Zhu, Y., Zhu, T., Liu, J. and Liu, W.: Investigations of
782 temporal and spatial distribution of precursors SO₂ and NO₂ vertical columns in the North
783 China Plain using mobile DOAS, Atmos. Chem. Phys., 18, 1535–1554, doi:10.5194/acp-2017-
784 719, 2017.

785 Wu, Z., Hu, M., Liu, S., Wehner, B., Bauer, S., Maßling, A., Wiedensohler, A., Petäjä T., Dal
786 Maso, M. and Kulmala, M.: New particle formation in Beijing, China: Statistical analysis of a
787 1-year data set, J. Geophys. Res., 112(D9), D09209, doi:10.1029/2006JD007406, 2007.

788 Xiao, S., Wang, M. Y., Yao, L., Kulmala, M., Zhou, B., Yang, X., Chen, J. M., Wang, D. F., Fu, Q.
789 Y., Worsnop, D. R. and Wang, L.: Strong atmospheric new particle formation in winter in
790 urban Shanghai, China, Atmos. Chem. Phys., 15(4), 1769–1781, doi:10.5194/acp-15-1769-
791 2015, 2015.

792 Yao, L., Garmash, O., Bianchi, F., Zheng, J., Yan, C., Kontkanen, J., Junninen, H., Mazon, S. B.,
793 Ehn, M., Paasonen, P., Sipilä M., Wang, M., Wang, X., Xiao, S., Chen, H., Lu, Y., Zhang, B.,
794 Wang, D., Fu, Q., Geng, F., Li, L., Wang, H., Qiao, L., Yang, X., Chen, J., Kerminen, V.-M.,
795 Petäjä T., Worsnop, D. R., Kulmala, M. and Wang, L.: Atmospheric new particle formation
796 from sulfuric acid and amines in a Chinese megacity, Science, 361(6399), 278–281,
797 doi:10.1126/science.aao4839, 2018.

798 Yue, D., Hu, M., Wu, Z., Wang, Z., Guo, S., Wehner, B., Nowak, A., Achtert, P., Wiedensohler, A.,
799 Jung, J., Kim, Y. J. and Liu, S.: Characteristics of aerosol size distributions and new particle
800 formation in the summer in Beijing, J. Geophys. Res. Atmos., 114(14), 1–13,
801 doi:10.1029/2008JD010894, 2009.

802 Zhang, Y. M., Zhang, X. Y., Sun, J. Y., Lin, W. L., Gong, S. L., Shen, X. J. and Yang, S.:
803 Characterization of new particle and secondary aerosol formation during summertime in
804 Beijing, China, Tellus, Ser. B Chem. Phys. Meteorol., 63(3), 382–394, doi:10.1111/j.1600-

805 0889.2011.00533.x, 2011.
806 Zheng, J., Khalizov, A., Wang, L. and Zhang, R.: Atmospheric pressure-ion drift chemical
807 ionization mass spectrometry for detection of trace gas species, *Anal. Chem.*, 82(17), 7302–
808 7308, doi:10.1021/ac101253n, 2010.
809 Zheng, J., Hu, M., Zhang, R., Yue, D., Wang, Z., Guo, S., Li, X., Bohn, B., Shao, M., He, L., Huang,
810 X., Wiedensohler, A. and Zhu, T.: Measurements of gaseous H₂SO₄ by AP-ID-CIMS during
811 CAREBeijing 2008 Campaign, *Atmos. Chem. Phys.*, 11(15), 7755–7765, doi:10.5194/acp-11-
812 7755-2011, 2011.
813 Zheng, J., Yang, D., Ma, Y., Chen, M., Cheng, J., Li, S. and Wang, M.: Development of a new
814 corona discharge based ion source for high resolution time-of-flight chemical ionization mass
815 spectrometer to measure gaseous H₂SO₄ and aerosol sulfate, *Atmos. Environ.*, 119, 167–173,
816 doi:10.1016/j.atmosenv.2015.08.028, 2015.
817

Table 1 Mean, median, 5-95 % percentiles of key atmospheric variables and [H₂SO₄] in the daytime.

	UVB (W m ⁻²)	[SO ₂] (ppbv)	CS (s ⁻¹)	[O ₃] (ppbv)	[HONO] (ppbv)	[NO _{x2}] (ppbv)	[H ₂ SO ₄] (× 10 ⁶ molecule cm ⁻³)	RH (%)
mean	0.17	4.6	0.11	10.5	0.74	25.3	5.4	28
median	0.14	3.7	0.11	9.0	0.51	23.0	4.9	26
5-95% percentiles	0.00-0.45	0.9-11.4	0.01-0.24	3.5-23.3	0.09-2.65	3.3-61.4	2.2-10.0	9-59

Table 2 Correlation coefficients (Spearman type) between [H₂SO₄] and atmospheric variables in the daytime. ~~Only correlation coefficients with p-values less than 0.01 are included to ensure a statistical significance.~~

	UVB	[SO ₂]	CS	[O ₃]	[HONO]	[NO ₂]	[H ₂ SO ₄]
UVB	1	0.01	-0.02	0.14	-0.23	-0.04	0.46
[SO ₂]		1	0.83	0.25	0.64	0.70	0.74
CS			1	0.36	0.75	0.77	0.60
[O ₃]				1	-0.02	-0.04	0.29
[HONO]					1	0.88	0.39
[NO ₂]						1	0.53
[H ₂ SO ₄]							1

Table 3 Proxy functions for the nonlinear fitting procedure.

Proxy	Function Equation [#]
N1	$k_0 \cdot UVB^a \cdot [SO_2]^b \cdot CS^c$
N2	$k_0 \cdot UVB^a \cdot [SO_2]^b$
N3	$k_0 \cdot UVB^a \cdot [SO_2]^b \cdot CS^c \cdot [O_3]^d$
N4	$k_0 \cdot UVB^a \cdot [SO_2]^b \cdot [O_3]^d$
N5	$k_0 \cdot UVB^a \cdot [SO_2]^b \cdot CS^c \cdot ([O_3]^d + [HONO]^e)$
N6	$k_0 \cdot UVB^a \cdot [SO_2]^b \cdot ([O_3]^d + [HONO]^e)$
N7	$k_0 \cdot UVB^a \cdot [SO_2]^b \cdot CS^c \cdot ([O_3]^d + [NO_{x2}]^f)$

[#]UVB is the intensity of ultraviolet radiation b in W cm⁻³; [SO₂] is the concentration of sulfur dioxide in molecule cm⁻³; CS is the condensation sink in s⁻¹; [O₃] is the concentration of ozone in molecule cm⁻³; [HONO] is the concentration of nitrous acid in molecule cm⁻³; [NO_{x2}] is the concentration of nitrogen dioxide in molecule cm⁻³; k_0 is a scaling factor.

Table 4 Results of the nonlinear fitting procedure for different proxy functions, together with correlation coefficient (R, Pearson type) and relative error (RE). ~~mean absolute error (MAE)~~.

Proxy	k_0	a	b	c	d	e	f	R	MAE ($\times 1$)
N1	515.74	0.14	0.38	0.03				0.83	20.04 1.03
N2	280.05	0.14	0.40					0.83	1.03 20.00
N3	9.95	0.13	0.39	-0.01	0.14			0.85	1.00 19.95
N4	14.38	0.13	0.38		0.14			0.85	1.00 19.95
N5	0.0072	0.15	0.41	-0.17	0.36	0.38		0.86	0.94 19.11
N6	2.38	0.14	0.33		0.24	0.24		0.85	0.98 19.66
N7	0.0013	0.13	0.40	-0.17	0.44		0.41	0.86	0.95 19.34

Figure Captions

Figure 1. Correlations (a) between $[\text{H}_2\text{SO}_4]$ and UVB intensity, and (b) between $[\text{H}_2\text{SO}_4]$ and $[\text{SO}_2]$ during the campaign from 9 February to 14 March, 2018. k_m is a constant term.

Figure 2. Correlation between $[\text{HONO}]$ and $[\text{NO}_{x2}]$ during the campaign from 9 February to 14 March, 2018. The black line represents a linear fitting with a zero intercept.

Figure 3. Performance assessments of proxy N2 and proxy N7. The REs are used to evaluate the performances of proxy N2 and N7, respectively as a function of linear bins of measured sulfuric acid concentrations. The averaged deviation and the relative deviation in the plots are defined by Eq. (6) and Eq. (7) and used to evaluate the performance of proxy N2 and N7, respectively. “Overlap” refers to the smaller values between proxy N2 and proxy N7, and the larger ones are indicated by the color code of proxies N2 and N7.

Figure 4. Comparison of measured $[\text{H}_2\text{SO}_4]$, $[\text{H}_2\text{SO}_4]_{\text{N2}}$, $[\text{H}_2\text{SO}_4]_{\text{N7}}$ and $[\text{H}_2\text{SO}_4]_{\text{Petäjä et al.}}$ on 10 March, 2018 with a time resolution of 5 min.

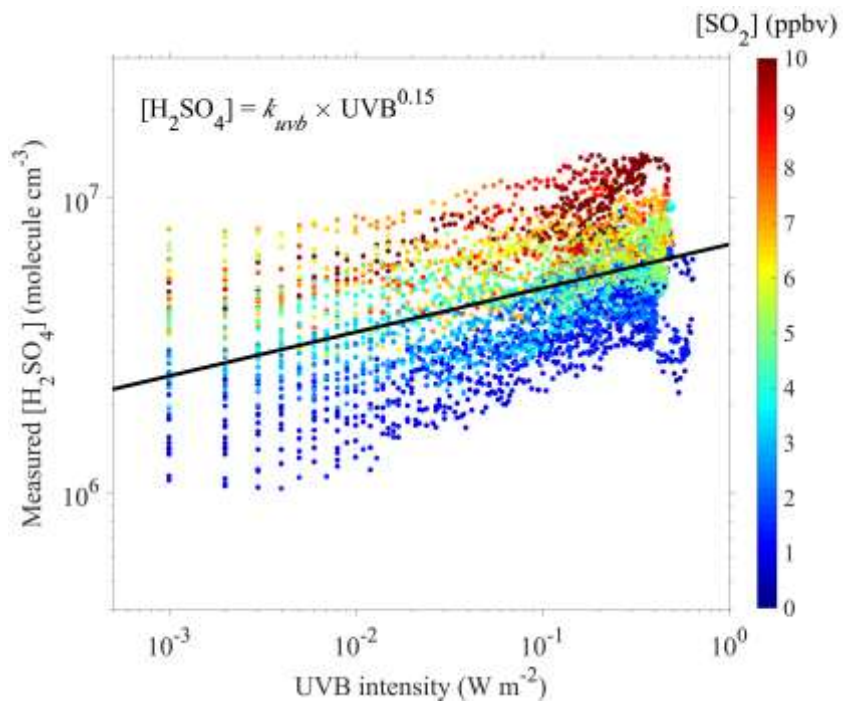


Figure 1a

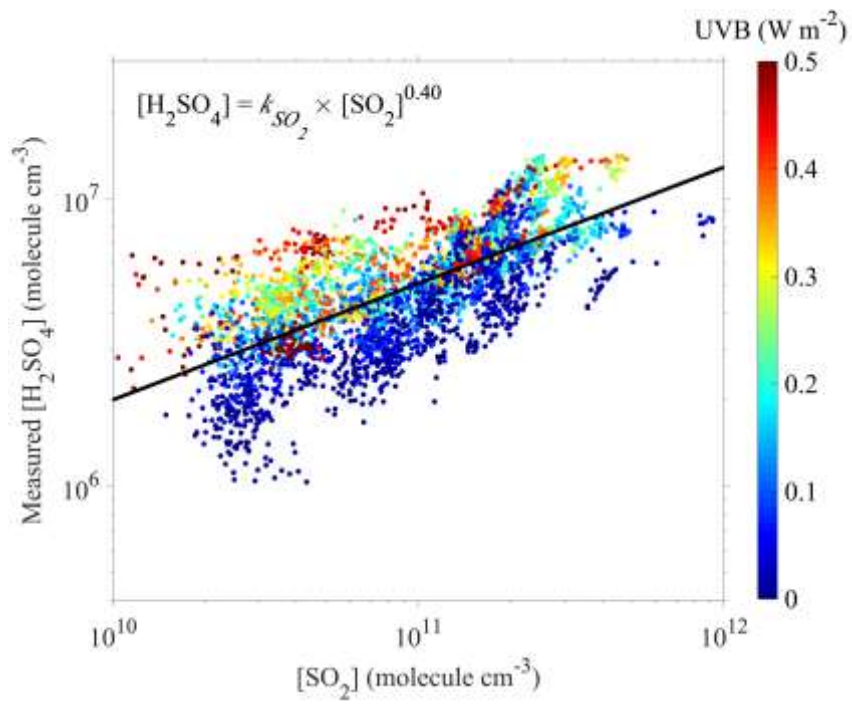


Figure 1b

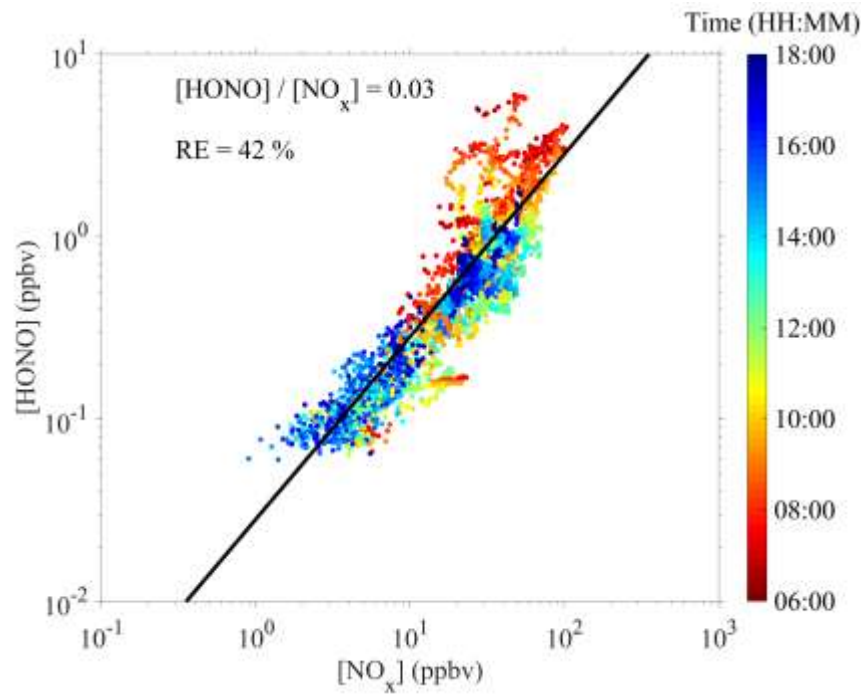


Figure 2

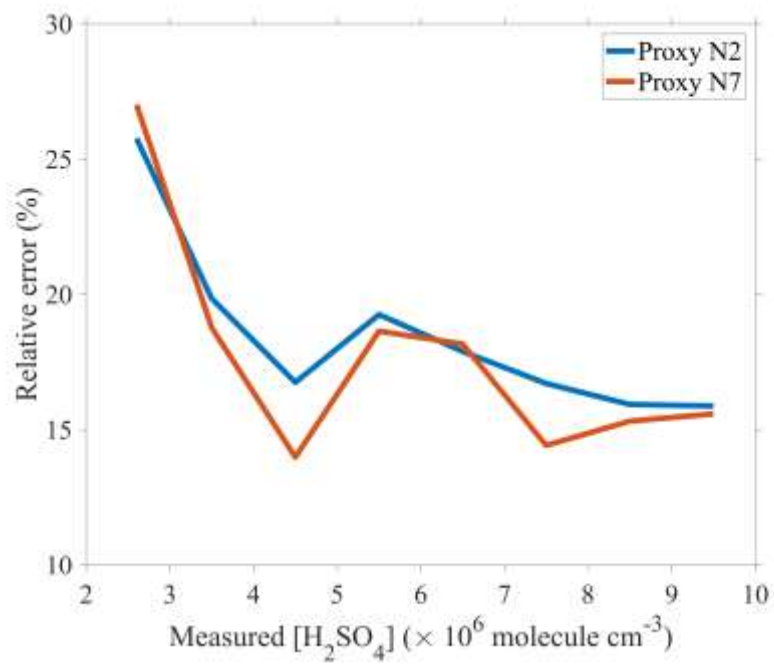


Figure 3a

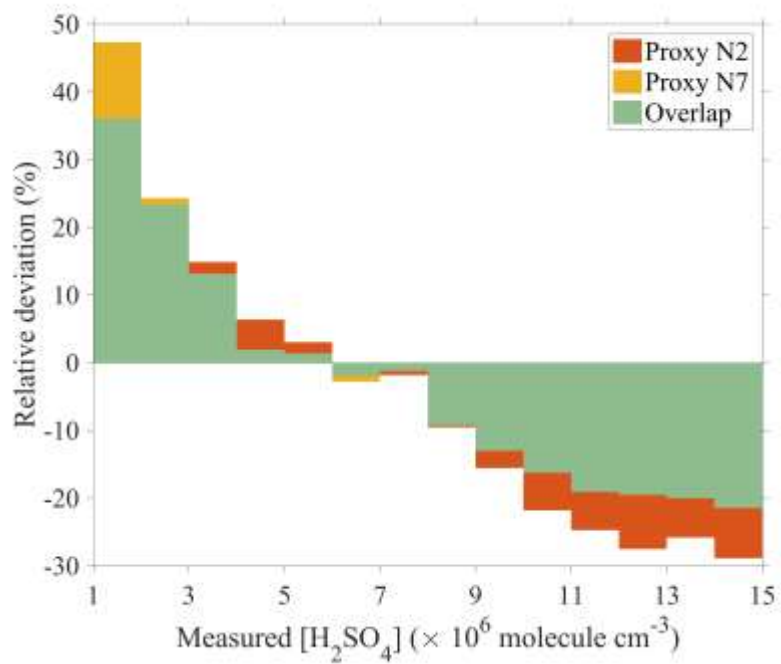


Figure 3b

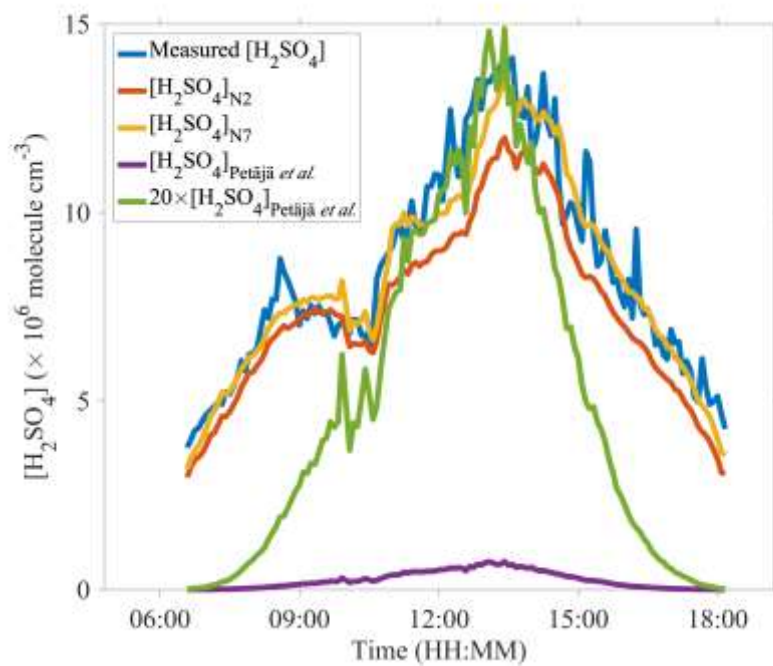


Figure 4